ACS OMEGA

http://pubs.acs.org/journal/acsodf

Article

Effect of Perfluoropolymers on the Anti-Wear Properties of Carbon Fiber/Polyphenylene Sulfide Composites: A Comparative Study

Xiaotao Qiu, Aiqun Gu,* Wenjian Tang, Siqi Tang, and Zili Yu*

Cite This: *ACS Omega* 2022, 7, 40316−40323

Read Online

ACCESS | Metrics & More | Article Recommendations | Supporting Information

ABSTRACT: In this work, several perfluoropolymers (PFP), including commercial polytetrafluoroethylene (PTFE), perfluorinated ethylene−propylene copolymer (FEP), tetrafluoroethylene-perfluoroalkyl vinyl ether copolymer (PFA), and irradiated PTFE (iPTFE) were used as additives to lubricate carbon fiber (CF)-reinforced polyphenylene sulfide (PPS) composites. The tribological properties of the yielding composites were studied and correlated with the melt processability of PFPs. Although the neat FEP and PFA have higher friction coefficients when compared with neat PTFE, the composites filled with FEP and PFA additives were found to exhibit a lower friction coefficient compared to PTFE at PFP content below 10 wt %. Moreover, the iPTFE-filled composites also showed similar results as FEP or PFA filled ones, very different from PTFE at low additions. Based on the morphological investigation, we postulate that FEP, PFA, and iPTFE are melt-kneaded with PPS due to their melt processability at processing temperature, leading to the good dispersion in composites in the form of smaller deformed spheres and/or fibril bands. The well-dispersion of PFPs in composites promotes the formation and growth of the transfer film on the counterface during sliding.

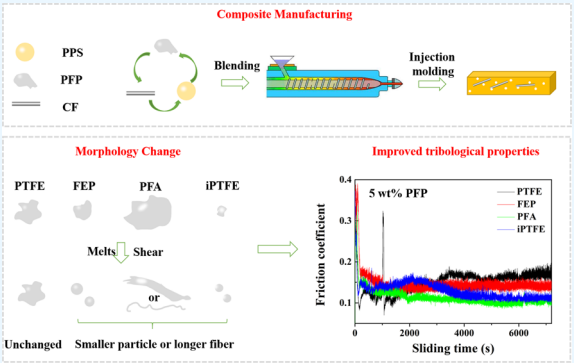

1. INTRODUCTION

Nowadays, polymer materials are playing an indispensable role in many fields,[1] and high-performance polymer composites are emerged increasingly by the addition of functional fillers.[2,3] Among various polymer composites, carbon fiber (CF)-reinforced polyphenylene sulfide (PPS) composites have been of interest for over decades due to their high strength, heat resistance, corrosion resistance, self-lubrication, and other excellent performances.[4−6] Thanks to the aforementioned advantages, CF-reinforced PPS composites have played a grand role in the fields of aerospace, machinery, and marine manufacture.[7,8] Nevertheless, owing to their relatively high friction coefficient and wear rate at high speeds and heavy loads, it is desired to improve the tribological properties of CF/PPS composites further by incorporating some solid lubricants.

As a typical representative of solid lubricants, polytetrafluoroethylene (PTFE) has attracted much attention for decades due to its very low friction coefficient.[9−13] For this reason, PTFE was widely used as a self-lubricant matrix or as an additive to prepare high-performance polymeric tribomaterials.[14−18] For instance, both powdery PTFE and fibrous PTFE have been proved to be effective in improving the tribological properties of PPS-based composites.[19−22] However, to the best of the authors' knowledge, PTFE is a hard-to-process polymer with extremely high melt viscosity (near zero melt flow rate), which limits its good dispersion as an additive in the matrix by conventional melt processing methods. To obtain effective self-lubrication, it is necessary to increase the amount of PTFE added, which may be detrimental to the overall performance (e.g., mechanical properties) of the manufactured composite.[23,24] Therefore, it is the pursuit of researchers to get balanced properties of PPS composites at low PTFE content by uniform dispersion. Achieving a homogeneous dispersion of PTFE in a matrix is attractive and challenging but not easy unless the PTFE is melt-processable. To reach the targets, many novel melt-processable PTFE-like perfluoropolymers (PFP) have been developed by introducing other perfluorinated monomers into the PTFE synthetic system. As a result, a series of new PFPs, such as the melt-processable perfluorinated ethylene−propylene copolymer (FEP) and tetrafluoroethylene-perfluoroalkyl vinyl ether copolymer (PFA), have been successfully prepared and commercialized and proved to have properties similar to PTFE.[25−27]

Received: August 18, 2022
Accepted: October 14, 2022
Published: October 26, 2022

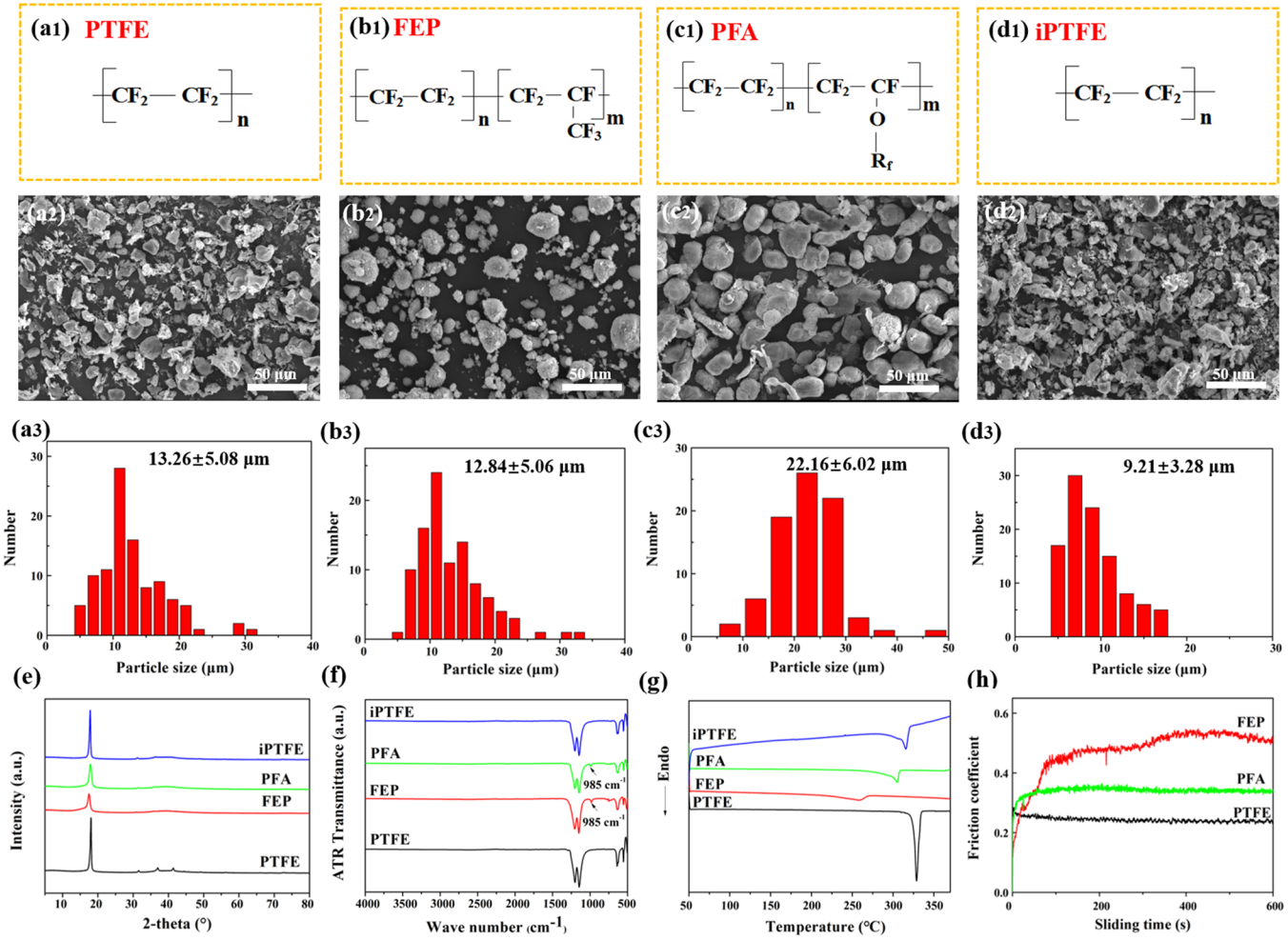

Figure 1. Characteristics of the PFPs. (a–d) molecular structure, morphology, and particle size distribution of PTFE (a1–a3), FEP (b1–b3), PFA (c1–c3), and iPTFE (d1–d3), respectively; (e) XRD patterns; (f) FT-IR spectra; (g) DSC curves; (h) transient friction coefficient.

Studies have shown that neat FEP and PFA performed higher friction coefficients when compared with PTFE due to their relatively irregular molecular chains.[28,29] Therefore, FEP and PFA have rarely been used to prepare self-lubricating components in place of PTFE but rather for other nonfriction fields such as insulating tubes or thin films, proton exchange membrane fuel cells,[30] and other electrochemical applications.[31] Moreover, few studies have been conducted so far on the tribological properties of composites filled with FEP and PFA as self-lubricant additives. Considering the melt processability of FEP and PFA, they are supposed to be well distributed in a thermal-resistant polymer matrix with high processing temperature, which then may give better tribological properties to the filled composites.

In the present work, nonmelt-processable PTFE and other three kinds of melt-processable PFPs, including FEP, PFA, and irradiated PTFE (iPTFE), were added into 30 wt % CF/PPS composites. The effect of PFP types and contents on the tribological behaviors of the composites was comprehensively investigated. This work aims to reveal the impact of melt processability of PFP on the tribological behaviors of the hybrid PPS composites and to gain more insight into the tribological mechanisms of PFP.

2. EXPERIMENTAL SECTION

2.1. Materials. The commercial PTFE (code 002A) is a product of Shanghai 3F New Material Co. Ltd., China. FEP is obtained from Zhejiang Jinhua Yonghe Fluorochemical Co., Ltd., China. PFA is provided by Daikin Co., Ltd., Japan. Irradiated PTFE (iPTFE) with melt processability was prepared by irradiating the PTFE (code 002A) under a 2 MGy dose.[32] According to their melt processability, PTFE is a nonmelt-processable PFP, and the other three (FEP, PFA, and iPTFE) are melt-processable PFPs. The rheological behaviors of the three melt-processable perfluoropolymers are shown in Figure S1. The characteristics of the four perfluoropolymers are collected in Figure 1. As indicated by the obvious crystallization peaks in the XRD pattern and melting peaks in the DSC curve, all four PFPs are crystalline polymers, and PTFE has the highest melting point. The friction coefficient of PFPs in Figure 1h indicates that PTFE has the lowest friction coefficient, and FEP has the highest one. The test was only carried out for 600 s because the worn volume of FEP was too large for a continuous test. In addition, it should be pointed out that the friction coefficient of iPTFE is not given because it could not be processed to a test specimen with sufficient mechanical strength.

PPS is purchased from Dunhuang Xiyu Special New Material Co., Ltd. (China). Short carbon fiber (CF, T-300)

https://doi.org/10.1021/acsomega.2c05298
ACS Omega 2022, 7, 40316−40323

with a diameter of 7 μm and length of 8 mm is a product of Weihai Guangwei Composite Co., Ltd. (China). The CF/PPS composite, one of the starting materials for the present work, was prepared by melt-kneading CF with PPS in a fixed CF/PPS weight ratio of 3/7.

2.2. Preparation of CF/PPS/PFP Composites. The mixture of CF/PPS composites with PFPs was melt blended on a twin-screw extruder (SJZS-10A, Wuhan Ruiming Plastic Machinery Co., Ltd., China) operated at temperatures of 310, 320, 330, and 320 °C in four zones along the screw direction. The blended mixtures were then injection molded to a 30 × 6 × 7 mm^3 testing specimen on an injection molding machine (SZS-20, Wuhan Ruiming Plastic Machinery Co., Ltd., China) at the barrel temperature of 320 °C and the mold temperature of 130 °C. The injection pressure was set at 0.5 MPa and maintained for 60 s.

2.3. Characterization. The tribological tests were carried out on a ring-on-block tester (M-200, Beijing Guance Testing Machine Co., Ltd., China) according to GB/T 3960−2016 (Chinese Standard), and the schematic diagram of the frictional pair is shown in Figure 2. The load and sliding speed applied to the specimen were 200 N and 200 rpm (0.42 m/s), respectively. The transient friction coefficient, average friction coefficient, and wear rate of the composites were calculated by the following formulas.

$$\mu = \frac{M}{R \times F} \tag{1}$$

where μ is the friction coefficient, M represents the friction torque (N·mm), R refers to the radius of the steel ring (mm), and F is the applied load to the test specimen (N).

$$V = d\left[\frac{\pi R^2}{180}\arcsin\left(\frac{b}{2R}\right) - \frac{b}{2}\sqrt{R^2 - \frac{b^2}{4}}\right] \tag{2}$$

$$Wv = \frac{V}{t} \tag{3}$$

where V represents the wear volume (mm^3), d is specimen width (mm), b is the width of worn scar (mm), R represents the steel ring radius (mm), Wv is the wear rate, and t is the sliding time (s).

Three specimens were tested for each sample, and the results were averaged to give the average friction coefficient and wear rate. Both the specimens and counterparts were thoroughly cleaned with ethanol before testing.

The worn and cryofractured surfaces of the CF/PPS/PFP composites, sputter-coated with a thin gold layer, were inspected using an SU3500 SEM (Hitachi, Japan) operated under 15 kV acceleration voltage. The elemental compositions of the cryofractured surface were also analyzed on an SEM equipped energy dispersive X-ray spectrometer (SEM−EDX, Oxford, UK). Attenuated total reflectance Fourier transform infrared spectrum (ATR-FT-IR) was detected on a Nicolet 6700 spectrometer (Thermo Fisher, USA), with a scan sum of 16 and a resolution of 2 cm^{-1}. The elements on the worn scar surface were characterized by an AXIS Ultra DLD X-ray photoelectron spectroscope (XPS, Kratos, UK). X-ray

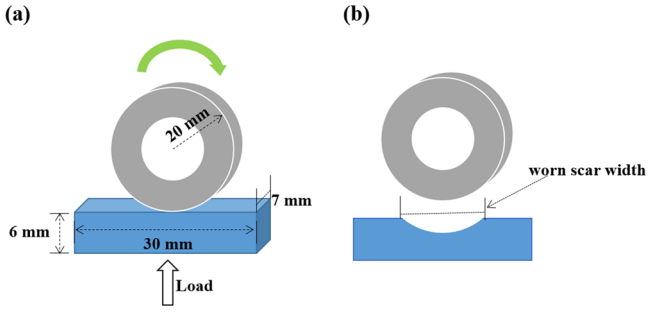

Figure 2. Schematic diagram of frictional pair (a) and specimen after friction (b).

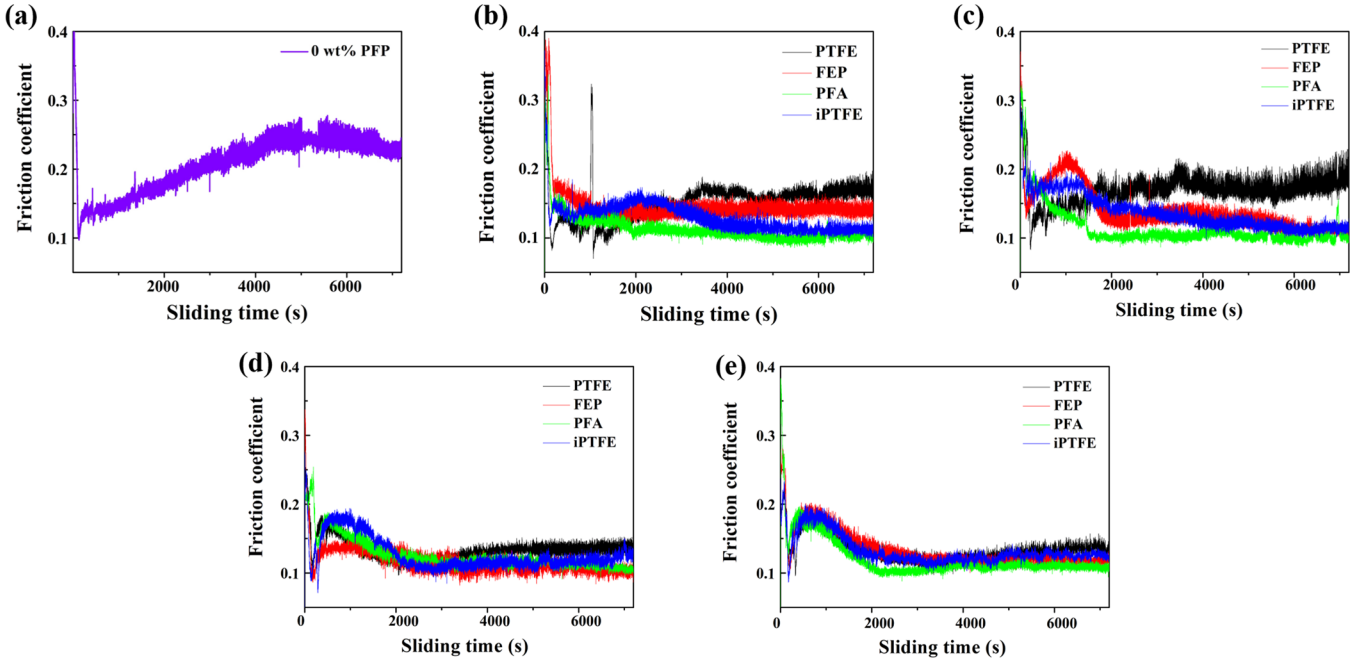

Figure 3. Transient friction coefficient of CF/PPS/PFP composites. (a) 0, (b) 5, (c) 10, (d) 15, and (e) 20 wt % PFP.

https://doi.org/10.1021/acsomega.2c05298
ACS Omega 2022, 7, 40316−40323

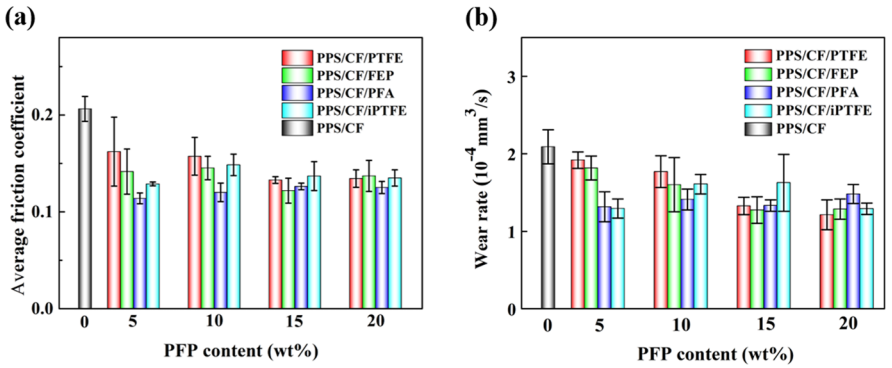

Figure 4. Tribological properties of CF/PPS/PFP composites. (a) Average friction coefficient; (b) wear rate.

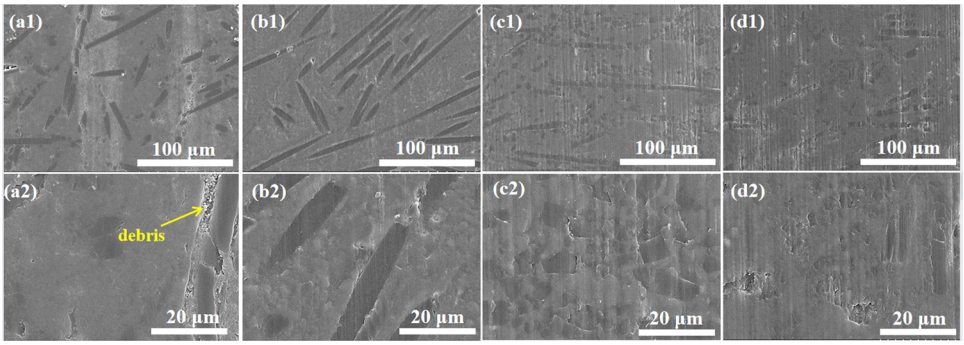

Figure 5. Worn scar SEM images of CF/PPS/5 wt % PFP composites. (a) PTFE, (b) FEP, (c) PFA, and (d) iPTFE.

diffraction (XRD) measurement was carried out on an Empyrean diffractometer (PANalytical, Netherlands).

3. RESULTS AND DISCUSSION

3.1. Tribological Properties. The transient friction coefficient of CF/PPS/PFP composites with different PFP contents is given in Figure 3. Figure 3a–e indicates that all specimens exhibit a remarkably high friction coefficient at the initial running-in stage. After that, composites filled with different PFPs show significant differences in the variation trend of the friction coefficient. During the stable friction period, the PTFE composite, as a reference, has a relatively high friction coefficient, while the composites filled with melt-processable PFPs (FEP, PFA, and iPTFE) exhibit a lower and more stable friction coefficient at a PFP content below 10 wt %. It is noticeable that the PFA-filled composite displays the lowest friction coefficient. With the increase of PFP addition, the friction coefficients of composites of four PFPs are gradually convergent. For example, the steady friction coefficient of PTFE composites is only slightly higher than the other PFP composites at the PFP addition of 15 wt % (Figure 3d), and the friction coefficient of four PFP composites are close to the same value at the PFP addition of 20 wt %.

For the sake of comparison, the average friction coefficient and wear rate of the composites were calculated and are shown in Figure 4. Although the neat FEP and PFA have a higher friction coefficient than the neat PTFE (Figure 1h), composites filled with FEP and PFA exhibit a lower average friction coefficient and wear rate than the PTFE composite at low PFP addition content (below 10 wt %), which is opposite to the performance of neat PFP. It is also noticed that the average friction coefficient and wear rate of iPTFE filled composites are lower than those of the PTFE-filled one at low PFP addition even though they have similar structures.

The above investigation indicates that the effect of PFP type on friction and wear properties of composites vary from remarkable (at 5 wt % PFP) to unobvious (at 20 wt % PFP), implying that the intensive distribution of PFP is achieved in the matrix in the latter case. In other words, PFP in the matrix alters from scattered or discrete (5 or 10 wt %) to dense distribution (20 wt %), and there is enough PFP on the frictional surface to lubricate each sliding surface of the steel ring at 20 wt % PFP addition (shown in Figure S2). In this case, the type of PFP is a less important factor for affecting lubrication, and the composites with different PFPs showed a similar friction coefficient. Further investigation concerning with the effect of PFP type on friction and wear properties becomes insignificant at much higher PFP content.

3.2. Tribological Mechanism. The aforementioned results suggest that the melt-processable PFPs (FEP, PFA, and iPTFE) seem to afford CF/PPS composites with better tribological properties at low content (below 10 wt %). To find out the origin of the anti-friction, the worn scar of composites containing 5 wt % PFP was measured by SEM and the images are shown in Figure 5. As depicted, the worn scar surfaces of all the composites are smooth without obvious plastic deformation, but there are also clear differences in the enlarged worn scar images. For the 5 wt % PTFE-modified composite (Figure 5a2), severe cracks and debris on its worn surface suggested that the major wear follows abrasive wear and fatigue wear mechanism. Whereas, the worn scars of CF/PPS composites filled with 5 wt % of melt-processable PFPs (FEP, PFA, iPTFE) display a smooth surface with little debris (Figure 5b–d), and the wear mechanism is presumed to be the slight abrasive wear.

https://doi.org/10.1021/acsomega.2c05298
ACS Omega 2022, 7, 40316–40323

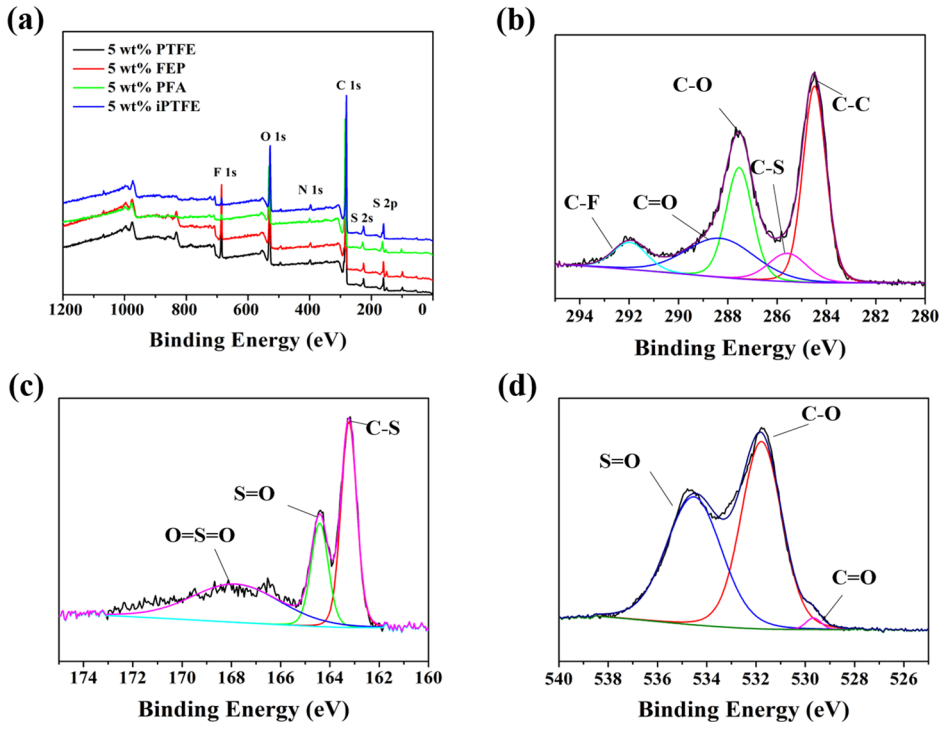

Figure 6. XPS spectra of the worn surface of CF/PPS/5 wt % PFP composites. (a) Wide scan, (b) C 1s of the 5 wt % PTFE composite, (c) S 2p of the 5 wt % PTFE composite, and (d) O 1s of the 5 wt % PTFE composite.

The elemental compositions of the worn surface were characterized by XPS, and the results are illustrated in Figure 6. As shown in Figure 6, the C, N, S, and F on the worn scar surface are consistent with elements of raw materials, while the high content of the O element on the worn surface does not exist in the raw materials. The high resolution spectra of C 1s, O 1s, and S 2p (in Figure 6b–d) indicate that the existence of O element is mainly related to the oxidation of C and S. Moreover, the results in Table 1 also show that the O/C ratio on the worn surface of the composites relies on the type of PFP. The O/C ratios of PFA and iPTFE composites are obviously lower than that of the PTFE composite, indicating that the composite with 5 wt % PTFE experienced more severe frictional oxidation reactions caused by high temperature during the friction process. In other words, the improved tribological performance of CF/PPS composites with melt-processable PFP (especially for PFA and iPTFE) is attributable to the alleviation of frictional drag, which well explains the reduction in the friction coefficient and wear rate at low PFP additions.

Table 1. Relative Content of C, O, S, and F on the Worn Surface of the 5 wt % PFP Composite (%)

PFP name	C	O	F	S	O/C
PTFE	70.73	16.49	5.46	7.32	23.31
FEP	71.48	16.74	6.37	5.42	23.42
PFA	81.38	13.00	0.74	4.88	15.97
iPTFE	78.81	14.27	0.71	6.21	18.11

The surface morphology and composition of the transfer films formed on the steel rings when rubbed with 5 wt % PFP composites were compared. As can be seen from Figure 7, the transfer film formed by PTFE composite is small and discrete, while the transfer film was larger and more continuous for FEP, PFA, and iPTFE composites. According to the formation mechanism of transfer film, the accumulated friction heat and interfacial shearing are responsible for the transfer and adhesion of the composite material on the surface of a steel ring.[22,33,34] The formed transfer film on the steel ring reduces the direct contact of the steel ring with the composite, thus reducing the continuous scraping of the steel ring to the composite. In this scenario, it is believed that the transfer film formed at the sliding interface drives a significant improvement in the tribological properties of the composites. As a result, for 5 wt % melt-processable PFP (FEP, PFA, and iPTFE)-filled composites, more transfer films are formed on the steel ring, which renders the composite with a lower friction coefficient and wear rate.

These results demonstrated that PFP types could influence the tribological properties and wear mechanism of the yielding composites at low PFP additions. Considering their different structures and melt processability, the cryofractured surfaces of CF/PPS/5 wt % PFP composites were observed (Figure 8), and a great morphological diversity emerged. PTFE in the composite retains its irregular morphology after melt processing, just like its original appearance in Figure 1a. However, the morphologies of melt-processable PFPs in their composites changed significantly compared to the original morphology. FEP and iPTFE existed as spheres or quasi-spheres in their composites, while PFA was in the form of flakes or fibers.

The above results proved that the morphology of PFP in its composites has a significant impact on the formation of transfer film and ultimately affects the tribological properties of composites. To the authors' knowledge, the morphology changes are mainly attributed to deformation caused by shear and/or flow during processing (sketched in Figure 9). PTFE, with the highest melting point and highest melt viscosity, performs like a solid filler that could withstand the processing

https://doi.org/10.1021/acsomega.2c05298
ACS Omega 2022, 7, 40316–40323

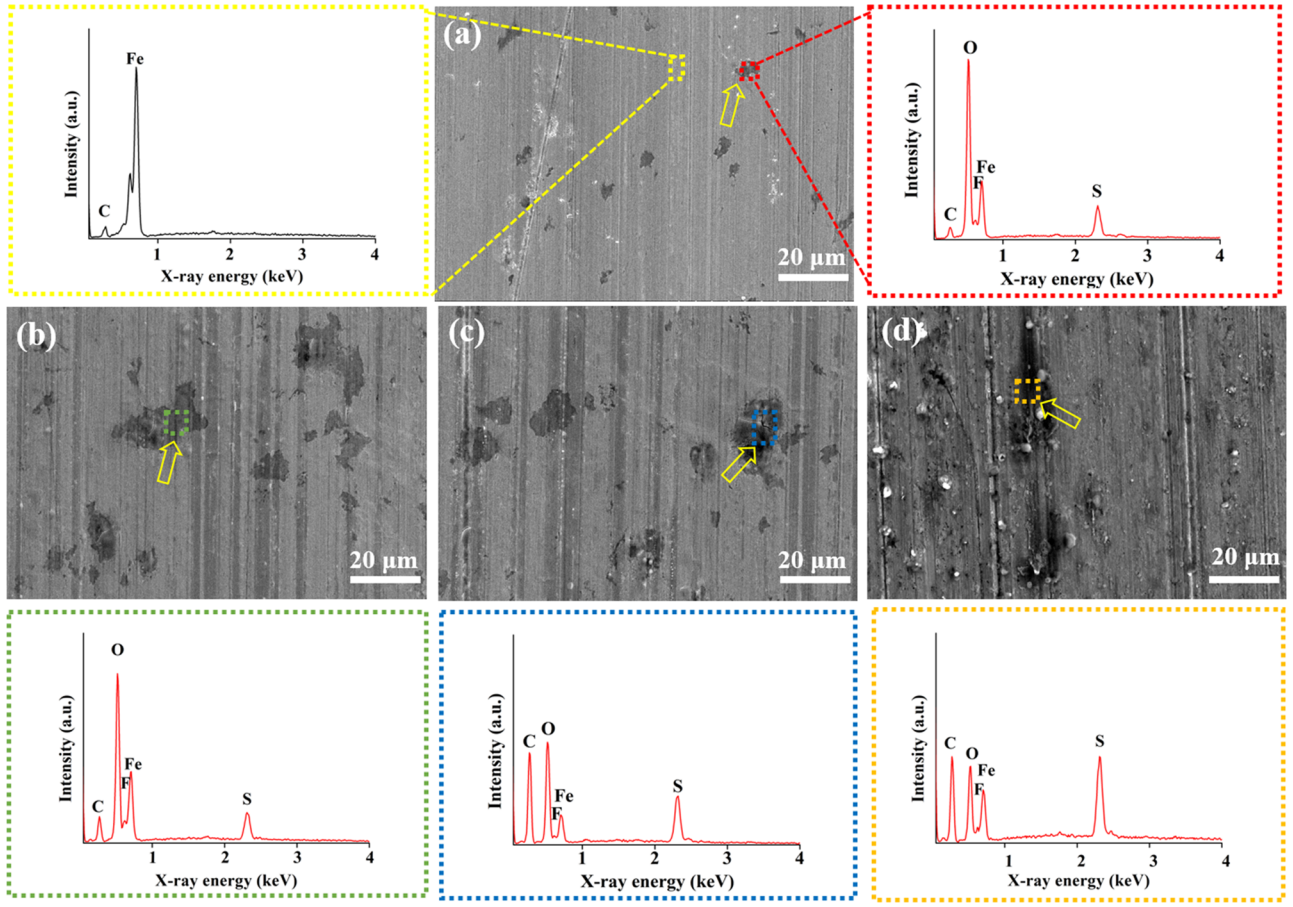

Figure 7. SEM images and EDS analysis of the steel ring sliding against CF/PPS/5 wt % PFP composites. (a) PTFE, (b) FEP, (c) PFA, and (d) iPTFE.

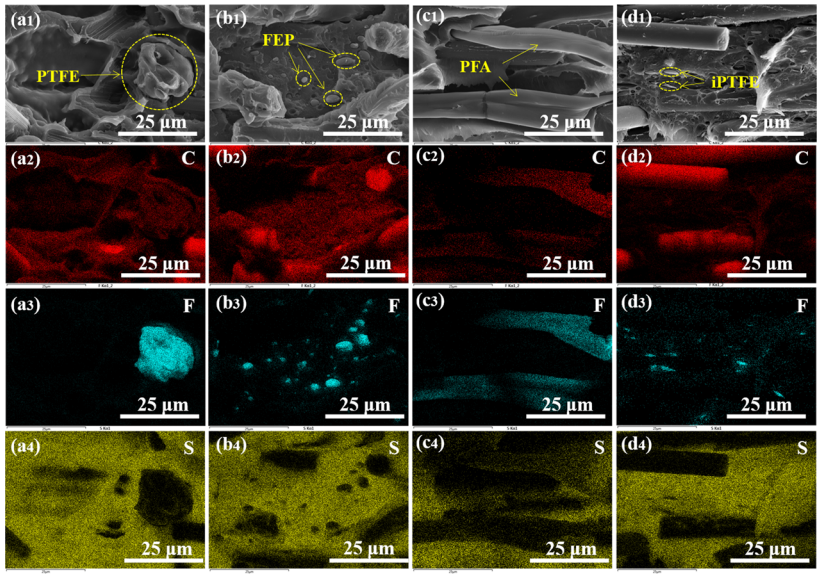

Figure 8. Cryofractured SEM images and the corresponding EDS mapping of CF/PPS/5 wt % PFP composites. (a) PTFE, (b) FEP, (c) PFA, and (d) iPTFE.

temperature and shear force during processing and consequently retains its original appearance in the composite. Melt-processable PFP particles (FEP, PFA, and iPTFE), however, could melt, deform or flow, and even break under shear force in melt processing because of their lower molecular weight and lower melting temperature. Upon release of shear force, the molten or deformed particles tend to aggregate again or recover to spherical solid during the cooling process. Therefore, melt-processable PFPs in composites are present in a spherical or quasi-spherical form (FEP, iPTFE) and a flaky or

https://doi.org/10.1021/acsomega.2c05298
ACS Omega 2022, 7, 40316−40323

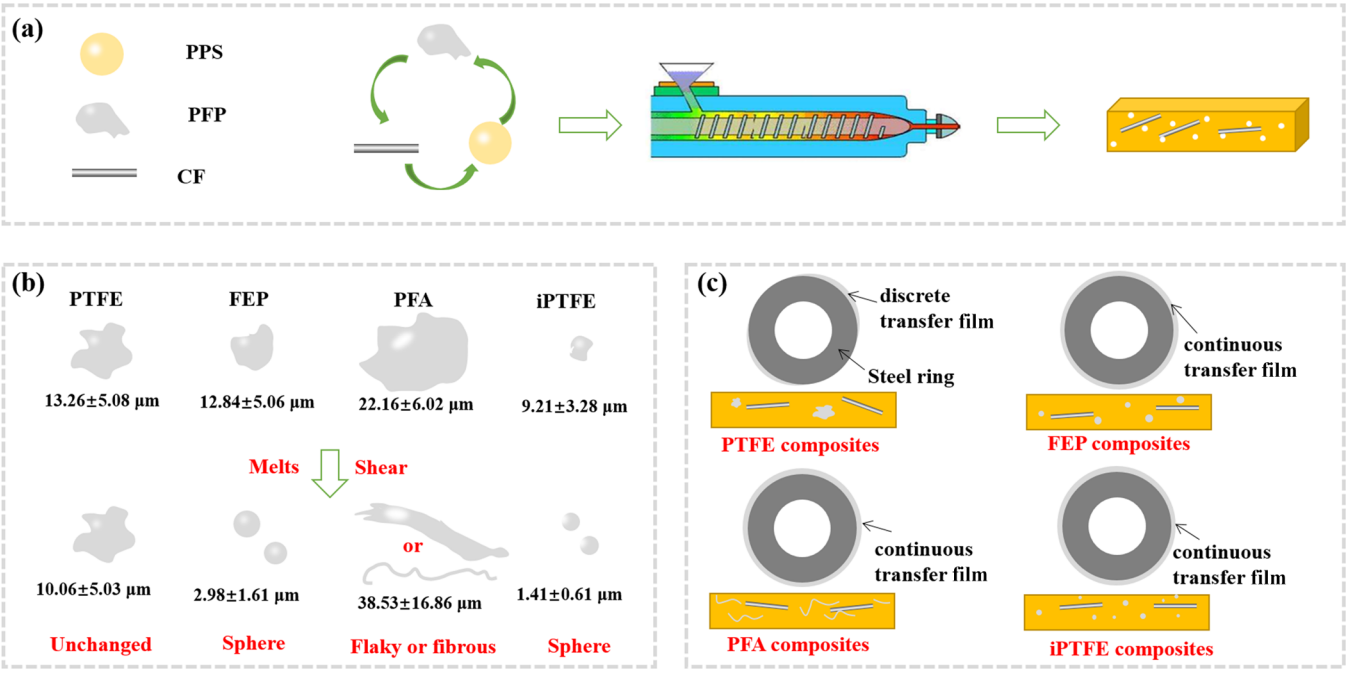

Figure 9. Schematic diagram of the fabrication process and tribo-film formation. (a) Fabrication process, (b) morphological changes of PFPs, and (c) tribo-film formation.

fibrous (PFA) shape, depending on melt-flow differences at processing conditions. Compared with their original particle, the condensed melt-processable PFPs appeared as the smaller particle and/or longer length strip (in Figure S3) in the PPS matrix. In other words, the melt-processable PFPs would have a larger specific area than their original ones after melt processing. The larger specific area means that melt-processable PFPs will be better dispersed in the matrix than PTFE, which effectively increases their contact area with the steel ring and promotes the formation of high-quality self-lubricating transfer films (in Figure 7b–d), resulting in the better self-lubricating properties.

4. CONCLUSIONS

In summary, PTFE and other three kinds of melt-processable PFP-filled CF/PPS composites were prepared by melt-blending, and their tribological properties were evaluated. From this study, the following conclusion could be drawn.

Although the friction coefficients of neat FEP and PFA are higher than that of PTFE, the friction coefficients of their filled composites are lower than that of the PTFE-filled material at low PFP addition (especially at 5 wt %). Similar results were shown for iPTFE filled composites.

The melt-processability of PFP is supposed to promote the dispersion of PFP in the PPS matrix, which favors the formation of transfer film, thereby reducing the friction coefficient and wear rate at low PFP addition. This work provides new strategies for the preparation of wear-resistant composites at high temperatures using melt-processable PFP as an additive.

■ ASSOCIATED CONTENT

Supporting Information

The Supporting Information is available free of charge at https://pubs.acs.org/doi/10.1021/acsomega.2c05298.

Melt viscosity of the melt-processable perfluoropolymer; SEM images of cryofractured surface of CF/PPS/PTFE composites with different PTFE contents; and SEM images of cryofractured surface of 5 wt % PFPs composites and PFP's particle size/length (PDF)

■ AUTHOR INFORMATION

Corresponding Authors

Aiqun Gu − *Analytical and Testing Center, Sichuan University, Chengdu 610064, China*; Email: gaq69@163.com

Zili Yu − *Analytical and Testing Center, Sichuan University, Chengdu 610064, China*; orcid.org/0000-0001-8697-3572; Email: ziliyu@163.com

Authors

Xiaotao Qiu − *Analytical and Testing Center, Sichuan University, Chengdu 610064, China*

Wenjian Tang − *Analytical and Testing Center, Sichuan University, Chengdu 610064, China*

Siqi Tang − *Analytical and Testing Center, Sichuan University, Chengdu 610064, China*

Complete contact information is available at: https://pubs.acs.org/10.1021/acsomega.2c05298

Author Contributions

Xiaotao Qiu: Conceptualization, Data curation, Formal analysis, Writing − original draft, review & editing. **Aiqun Gu**: Writing − review & editing. **Wenjian Tang**: Writing − review. **Siqi Tang**: Writing − review. **Zili Yu**: Supervision, Writing − review & editing.

Notes

The authors declare no competing financial interest.

https://doi.org/10.1021/acsomega.2c05298
ACS Omega 2022, 7, 40316−40323

■ ACKNOWLEDGMENTS

We thank the Analytical and Testing Center of Sichuan University for providing SEM observations. Thanks are especially given to Yi He for his kindly help in SEM images.

■ REFERENCES

(1) Liu, W.; Wu, X.; Chen, X.; Liu, S.; Zhang, C. Flexibly controlling the polycrystallinity and improving the foaming behavior of polylactic acid via three strategies. *ACS Omega* **2022**, *7*, 6248.
(2) Liu, W.; Wu, X.; Liang, J.; Ding, P.; Lv, Y.; Zhang, C. Preparation of antibacterial and strengthened high-density polyethylene composites via compounding with silver ion glass microbead-loaded basalt fiber. *J. Mater. Eng. Perform.* **2022**, *31*, 1493.
(3) Liu, W.; Wu, X.; Ou, Y.; Liu, H.; Zhang, C. Electrically conductive and light-weight branched polylactic acid-based carbon nanotube foams. *e-Polym.* **2021**, *21*, 96.
(4) Parker, M.; Inthavong, A.; Law, E.; Waddell, S.; Ezeokeke, N.; Matsuzaki, R.; Arola, D. 3D printing of continuous carbon fiber reinforced polyphenylene sulfide: Exploring printability and importance of fiber volume fraction. *Addit. Manuf.* **2022**, *54*, No. 102763.
(5) Kim, M.; Lee, J.; Cho, M.; Kim, J. Improvement of thermal and abrasion resistance performance of polyphenylene sulfide composite through 3-mercaptopropyl trimethoxysilane treatment of carbon fiber and graphene oxide fillers. *Polym. Test.* **2022**, *108*, No. 107517.
(6) André, N. M.; Bouali, A.; Maawad, E.; Staron, P.; dos Santos, J. F.; Zheludkevich, M. L.; Amancio-Filho, S. T. Corrosion behavior of metal−composite hybrid joints: Influence of precipitation state and bonding zones. *Corros. Sci.* **2019**, *158*, 108075.
(7) Stoeffler, K.; Andjelic, S.; Legros, N.; Roberge, J.; Schougaard, S. B. Polyphenylene sulfide (PPS) composites reinforced with recycled carbon fiber. *Compos. Sci. Technol.* **2013**, *84*, 65−71.
(8) Luo, W.; Liu, Q.; Li, Y.; Zhou, S.; Zou, H.; Liang, M. Enhanced mechanical and tribological properties in polyphenylene sulfide/polytetrafluoroethylene composites reinforced by short carbon fiber. *Composites, Part B* **2016**, *91*, 579−588.
(9) Biswas, S. K.; Vijayan, K. Friction and wear of PTFE — a review. *Wear* **1992**, *158*, 193−211.
(10) Wang, Y.; Yan, F. Tribological properties of transfer films of PTFE-based composites. *Wear* **2006**, *261*, 1359−1366.
(11) Yang, Y.; Wang, H.; Ren, J.; Gao, G.; Zhao, G.; Chen, S.; Wang, N.; Wang, J. Multi-environment adaptability of self-lubricating core/shell PTFE@PR composite: Tribological characteristics and transfer mechanism. *Tribol. Int.* **2021**, *154*, No. 106718.
(12) Chen, Z.; Wu, Z.; Sun, J.; Mao, C.; Su, F. Improved load-bearing capacity and tribological properties of PTFE coatings induced by surface texturing and the addition of GO. *Tribol. Lett.* **2021**, *69*, 47.
(13) Li, X.; Wu, S.; Ling, Y.; Zhang, C.; Luo, J.; Dai, Y. Preparation and tribological properties of PTFE/DE/ATF6 composites with self-contained solid-liquid synergetic lubricating performance. *Compos. Commun.* **2020**, *22*, No. 100513.
(14) Voort, J. V.; Bahadur, S. The growth and bonding of transfer film and the role of CuS and PTFE in the tribological behavior of PEEK. *Wear* **1995**, *181-183*, 212−221.
(15) Xie, C.; Wang, K. Synergistic modification of the tribological properties of polytetrafluoroethylene with polyimide and boron nitride. *Friction* **2021**, *9*, 1474−1491.
(16) Bijwe, J.; Sen, S.; Ghosh, A. Influence of PTFE content in PEEK−PTFE blends on mechanical properties and tribo-performance in various wear modes. *Wear* **2005**, *258*, 1536−1542.
(17) Jotaki, K.; Miyatake, M.; Stolarski, T.; Sasaki, S.; Yoshimoto, S. Tribological performance of natural resin urushi containing PTFE. *Tribol. Int.* **2017**, *113*, 291−296.
(18) Zhou, S.; Wu, Y.; Zou, H.; Liang, M.; Chen, Y. Tribological properties of PTFE fiber filled polyoxymethylene composites: The influence of fiber orientation. *Compos. Commun.* **2021**, *28*, No. 100918.
(19) Luo, Z.; Zhang, Z.; Wang, W.; Liu, W. Effect of polytetrafluoroethylene gradient-distribution on the hydrophobic and tribological properties of polyphenylene sulfide composite coating. *Surf. Coat. Technol.* **2009**, *203*, 1516−1522.
(20) Shi, Y.; Zhou, S.-T.; Heng, Z.-G.; Liang, M.; Wu, Y.; Chen, Y.; Zou, H. W. Interlocking structure formed by multiscale carbon fiber−polytetrafluoroethylene fiber hybrid significantly enhances the friction and wear properties of polyphenylene sulfide based composites. *Ind. Eng. Chem. Res.* **2019**, *58*, 16541−16551.
(21) Shi, Y.; Liang, M.; Zou, H.; Zhou, S.; Chen, Y. In situ microfibrillation of polyamide 66 and construction of ordered polytetrafluoroethylene fibers to significantly reduce the friction coefficient of polyphenylene sulfide. *Ind. Eng. Chem. Res.* **2021**, *60*, 281−290.
(22) Shi, Y.; Zhou, S.; Zou, H.; Liang, M.; Chen, Y. In situ microfibrillization and post annealing to significantly improve the tribological properties of polyphenylene sulfide/polyamide 66/polytetrafluoroethylene composites. *Composites, Part B* **2021**, *216*, No. 108841.
(23) Zhang, X.; Liao, G.; Jin, Q.; Feng, X.; Jian, X. On dry sliding friction and wear behavior of PPESK filled with PTFE and graphite. *Tribol. Int.* **2008**, *41*, 195−201.
(24) Qiu, X.; Fu, C.; Gu, A.; Gao, Y.; Wang, X.; Yu, Z. Preparation of high-performance PEEK anti-wear blends with melt-processable PTFE. *High Perform. Polym.* **2020**, *32*, 645−654.
(25) Chen, B.; Wang, J.; Yan, F. Microstructure of PTFE-based polymer blends and their tribological behaviors under aqueous environment. *Tribol. Lett.* **2012**, *45*, 387−395.
(26) Crosby, J. M.; Carreno, C. A.; Talley, K. L. Melt processible fluoropolymer composites. *Polym. Compos.* **1982**, *3*, 97−101.
(27) Bowers, R. C.; Zisman, W. A. Frictional properties of tetrafluoroethylene-perfluoro (propyl vinyl ether) copolymers. *Ind. Eng. Chem. Prod. Res. Dev.* **1974**, *13*, 115−118.
(28) Sidebottom, M. A.; Pitenis, A. A.; Junk, C. P.; Kasprzak, D. J.; Blackman, G. S.; Burch, H. E.; Harris, K. L.; Sawyer, W. G.; Krick, B. A. Ultralow wear Perfluoroalkoxy (PFA) and alumina composites. *Wear* **2016**, *362-363*, 179−185.
(29) Menzel, B.; Blanchet, T. A. Enhanced wear resistance of gamma-irradiated PTFE and FEP polymers and the effect of post-irradiation environmental handling. *Wear* **2005**, *258*, 935−941.
(30) Mariani, M.; Basso Peressut, A.; Latorrata, S.; Balzarotti, R.; Sansotera, M.; Dotelli, G. The role of fluorinated polymers in the water management of proton exchange membrane fuel cells: A review. *Energies* **2021**, *14*, 8387.
(31) Nasef, M.; Saidi, H.; Nor, H.; Foo, O. M. Cation exchange membranes by radiation-induced graft copolymerization of styrene onto PFA copolymer films II. Characterization of sulfonated graft copolymer membranes. *J. Appl. Polym. Sci.* **2000**, *76*, 1−11.
(32) Fu, C.; Yu, X.; Zhao, X.; Wang, X.; Gu, A.; Xie, M.; Chen, C.; Yu, Z. Mechanistic insights into the room temperature transitions of polytetrafluoroethylene during electron-beam irradiation. *Nucl. Instrum. Methods Phys. Res., Sect. B* **2017**, *410*, 188−192.
(33) Onodera, T.; Park, M.; Souma, K.; Ozawa, N.; Kubo, M. Transfer-film formation mechanism of polytetrafluoroethylene: A computational chemistry approach. *J. Phys. Chem. C* **2013**, *117*, 10464−10472.
(34) Shen, J. T.; Pei, Y. T.; De Hosson, J. T. M. Structural changes in polytetrafluoroethylene molecular chains upon sliding against steel. *J. Mater. Sci.* **2014**, *49*, 1484−1493.

https://doi.org/10.1021/acsomega.2c05298
ACS Omega 2022, 7, 40316−40323